Heliyon 9 (2023) e18189

Contents lists available at ScienceDirect

Heliyon

journal homepage: www.cell.com/heliyon

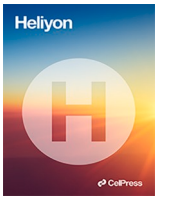

Assessment of soil respiration process in a mangrove swamp of Panama's Bay

Natasha Alejandra Gómez [a], Lilisbeth Rodríguez [a], Francisco Ramón López Serrano [b], Reinhardt Pinzón [c,d,e,*]

[a] Universidad Tecnológica de Panamá, Facultad de Ingeniería Civil, Panama
[b] Higher Technical School of Agricultural and Forest Engineering, University of Castilla-La Mancha, Campus Universitario s/n, 02071 Albacete, Spain
[c] Universidad Tecnológica de Panamá, Centro de Investigaciones Hidráulicas e Hidrotécnicas (CIHH), Grupo de Computación de Alto Rendimiento, Panama
[d] Sistema Nacional de Investigación (SNI), SENACYT, Panama
[e] Centro de Estudios Multidisciplinarios en Ciencias, Ingeniería y Tecnología (CEMCIT-AIP), Panama

ARTICLE INFO

Keywords:
Wetlands
Land flow
Coast of Panama
Climate change
Linear multiple regression
CO_2 flux

ABSTRACT

Studies reveal that mangroves have the ability to store underground carbon more than a tropical forest, and this function is classified as the second most important to mitigate the effects of climate change. However, part of the carbon fixed returns to the atmosphere, and this is done through soil respiration. The present study seeks to quantify the total soil efflux (a subrogate of total soil respiration) that includes both autotrophic and heterotrophic soil efflux, emitted by a Panama's mangrove swamp, as well as to investigate what drivers are important. Firstly, 3 plots were established with predominant mangroves species, such as salty mangrove tree (*Avicennia bicolor Standl.*) and black mangrove tree (*Avicennia germinans* L.). Secondly, a forest inventory was carried out in one ha, resulting in 371 trees ha^{-1}, where the salty mangrove tree prevailed with 219 individuals in front of the black mangrove tree, with 152 trees. In addition, tree level measurements were performed such as diameter at breast height (DBH), crown diameter and distance between trees. Third, using a Licor 6400XT infrared gas analyzer system and a meteorological tower, soil CO_2 fluxes and air and soil temperature were measured respectively. Results showed a total of 33.61 t of CO_2 ha^{-1} emitted by the soil of the mangrove in 3.5 months.

1. Introduction

Climate change is a global phenomenon that has had a growing scientific, political, social and media interest because its repercussions harm and modify practically all human activities. Likewise, it alters the functioning of the biosphere and the integrity of ecosystems as a whole, with varied impacts on the vital support of biogeochemical cycles [1].

Currently, climate change is affected by the high emissions of greenhouse gases derived from anthropogenic activities, causing alterations in the atmosphere [2]. Some of the existing problems on the part of human activities within the wetlands are the illegal

* Corresponding author. Universidad Tecnológica de Panamá, Centro de Investigaciones Hidráulicas e Hidrotécnicas (CIHH), Grupo de Computación de Alto Rendimiento, Panama.
E-mail address: reinhardt.pinzon@utp.ac.pa (R. Pinzón).

https://doi.org/10.1016/j.heliyon.2023.e18189
Received 9 January 2023; Received in revised form 10 July 2023; Accepted 11 July 2023
Available online 11 July 2023

felling of mangroves, movement of land without authorization and the accumulation of solid waste due to population growth.

Wetlands are characterized by being an ecosystem with soils saturated with water, permanently or temporarily, because they are located in areas where seawater mixes with freshwater that flows from rivers. Among the best-known coastal wetlands, it is included the mangroves, which are made up of groups of trees called mangroves, and it is common to see them in tropical or subtropical areas.

Mangroves swamp can be defined as diverse ecosystems with a set or group of trees, shrubs, bushes, some ferns and/or palm trees where the main member is the mangrove tree, which only grow on tropical and subtropical coastlines, thus being able to grow in salt water [3].

It is estimated that mangroves occupy only 3% of the earth's surface [3]. It offers us important services such as: artisanal fishing, industrial fishing in the exclusive economic zone, ecological tourism, water purification, protection against storms, tidal waves, and floods and, last but not least, high capacity as carbon sinks and reservoirs [4].

There are at least 68 species of mangrove worldwide [5]. However, its center of diversity is the Indo-Pacific region, where 52 mangrove species were recorded [5]. In the American continent there are only about 10 species, among some of them we have the black mangrove (*Avicennia germinans* L.), red mangrove (*Rhizophora mangle*), white mangrove (*Laguncunaria racemosa*), buttonwood mangrove (*Conocarpus erectus*), salty mangrove (*Avicennia bicolor Standl.*) and yellow mangrove (*Rhizophora harrisonii*) [5].

The estimated coverage of mangroves in the world is between 14 and 24 million hectares [5]. But through recent calculations that indicate more real values, it is estimated that it is closer to the estimated minimum of 13.8 million ha, which is related to the improvement in measurement techniques and associated with losses due to deforestation and conversion of areas of mangrove The largest mangrove areas are found in Asia, with 6.8 million hectares, which represents between 34 and 42% of the world total. Indonesia contains almost 23% of the world's mangroves, followed by Africa (20%), North and Central America (15%), Oceania (12%), South America (11%) and Australia (7%). The mangroves of Southeast Asia are the most developed and probably the most diverse in the world 64% of all mangroves in the world are found in 10 countries and 42% are concentrated in just four countries: Indonesia, Brazil, Australia, and Mexico [5].

However, this ecosystem has an important role in mitigating climate variability. Thanks to its composition, they are the most effective sinks of carbon dioxide (main greenhouse gas) on the planet [6]. Mangroves fix large amounts of carbon in biomass through photosynthesis that accumulates in both vegetation and the soil [7,8].

The mangrove swamp of Panama' Bay has been designated as a protected area, for being of great value to humanity, and being of international importance, it is known as a Ramsar Site, by the Ramsar Convention (International Agreement that promotes the conservation and wise use of wetlands) since 2003 [9].

Because of the advantageous physical, chemical, and hydrological characteristics of soil organic matter for tree growth, forest soil experts have long recognized its significance. The majority of the soil carbon is found in the mineral soil, which is one of the organic layers made up of fine and coarse woody decomposition of detritus. Due to the significant amount of carbon in the soil, forest soils are a crucial part of the global carbon cycle [10].

A straightforward Q_{10} or Arrhenius function is most frequently used to estimate the soil surface CO_2 flux (S), which is the sum of root and heterotrophic respiration [10]. Some of the variation may be the result of methodological variations. Moisture, substrate

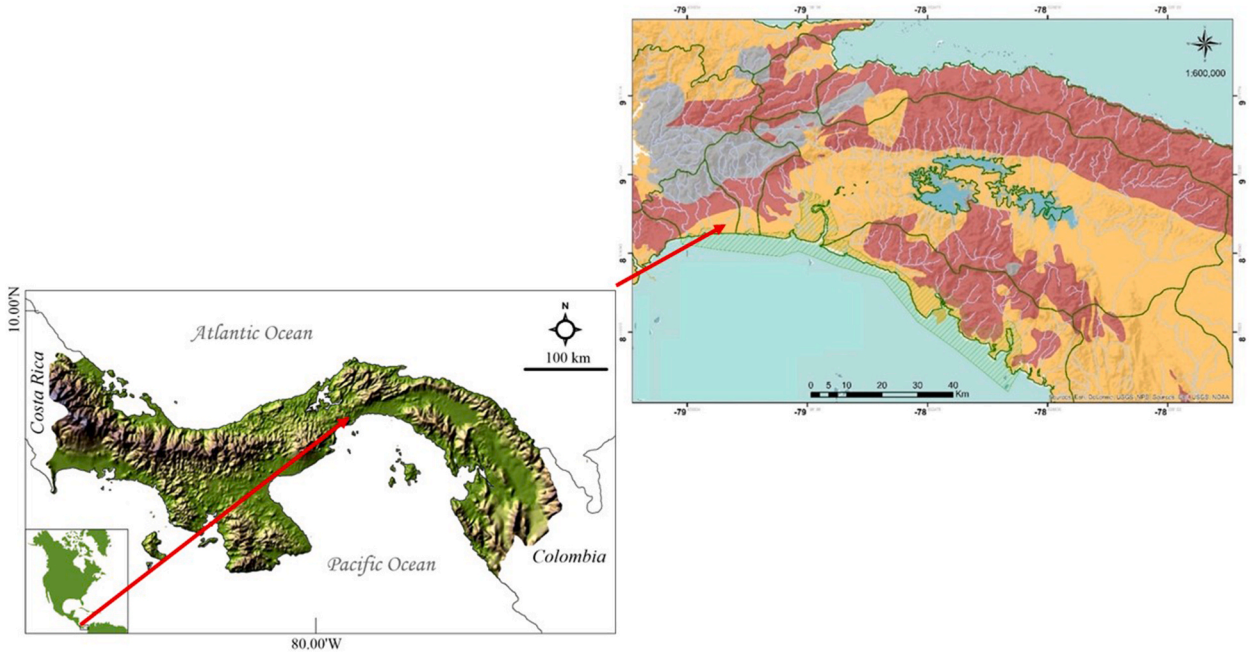

Fig. 1. Geology of coastal basins with delta in the Panama Bay Wetland [[15]].

quality, fine root dynamics, and population and community dynamics of soil microorganisms are additional significant factors that affect S [10].

On a larger scale, distinct plant communities frequently exhibit variable rates of soil respiration, and overall soil respiration varies between ecosystems. In addition to its impact on the soil's microclimate and structure, the type of vegetation also has an impact on how much litter is deposited in the soil and how actively the roots grow. The current forest species composition may change as a result of climate change, necessitating adaptation owing to changes in soil conditions including moisture content and temperature regime, which would affect soil respiration. It's crucial to comprehend how each site reacts in order to assess the effects of climate change on CO_2 flux at the ecosystem level [11,12].

The general goal of this study seeks to quantify the total soil respiration (S, autotrophic and heterotrophic) as well as the drivers that control its behavior [13] in the Panama's mangrove swamp.

2. Materials and methods

2.1. Study site

The Panama Bay wetland is made up of a set of ecosystems that includes mangrove forests, mudflats, estuaries, adjacent freshwater marshes, and shallow marine waters; This is located south of the province of Panama, extending from west to east from the Caimito River (Panama District) to the Santa Bárbara River (Chimán District) [14,15]. The total protected area has an extension of 87,226.8 ha of which 39,703.6 ha correspond to land surface and 45,960.9 ha form part of the marine surface of the Bay of Panama, which has a total length of 61.36 nautical miles, in addition to including a buffer zone of 50 m between the largest land surface in the area and the adjoining land [9]. Fig. 1 shows the geological map of Panama, scale 1:250,000, tells us that, once the isthmus was consolidated, it was consolidated in volcanic, plutonic, metamorphic, and sedimentary rocks. In the area of the Panama Bay Wetland, volcanic and sedimentary formations predominate; however, to the north of the hydrological basins with delta in the wetland mangroves formations of plutonic origin are identified. The mangrove soil is classified as organic, formed by the high accumulation of organic remains characterized by having little content of clay, silt and sand, they are maintained by anaerobic processes and the nutrients are released by the decomposition of organic matter in aerobic zones. , with continuous remineralization; and inorganic, formed by silt and clay deposits in alluvial plains, these are defined as terraces of sediments that are deposited along the riverbed as a product of erosion [15].

On the Panamanian coast, where seasonality is less pronounced and annual rainfall ranges from 2100 to 6400 mm, mangrove trees exceed 35 m in height and biomass of 280 tha^{-1} [15]. These mangroves are made up of red mangrove tree (*Rhizophora racemosa* and *Rhizophera mangle*) salt mangrove tree (*Avicennia bicolor Standl.*) (Fig. 2), black mangrove (*Avicennia germinans* L.) (Fig. 3), white mangrove (*Laguncularia racemosa*), piñuelo mangrove (*Pelliciera rhizophorae*) and mangrove ferns (*Acrostichum aureum* and *Acrostichum danaeifolium*) [15].

Fig. 2. *Avicennia bicolor Standl.*

Fig. 3. *Avicennia germinans* L. [[3]].

2.2. Methodology

2.2.1. General experiment description

The general methodology consists of estimating the projected crown coverage area by mangrove trees (Cct, m^2) and the area corresponding to bare soil (BS, m^2), and applying the total soil respiration models (efflux, see 2.2.2 section) independently to both types of surface (bare soil and soil under trees). This is since it has been shown [16] that there is a decreasing gradient in efflux magnitude from the tree to outside the crown area projection. To quantify the Cct and BS areas, a representative mangrove plot of 1 ha (100 × 100 m) was selected, where a classic inventory was carried out. In this plot all diameters at breast height (DBH, cm) were measured (Fig. 4). After, we carried out an experiment for SR (efflux) measurement following a linear transect starting from a tree, in three subplots (5 × 5 m on size, Fig. 5) using a portable infrared gas analyzer coupled to a soil CO_2 flux chamber (Li-6400XT and 6400-09, respectively; Li-Cor, Lincoln, NE, USA). Next two SR models were defined depending on the soil type (bare soil and soil under the crown trees). Finally, we scaled to the total population (the hectare) in base to the different type of soil covert.

Fig. 4. Diameter measurement at breast height (DBH).

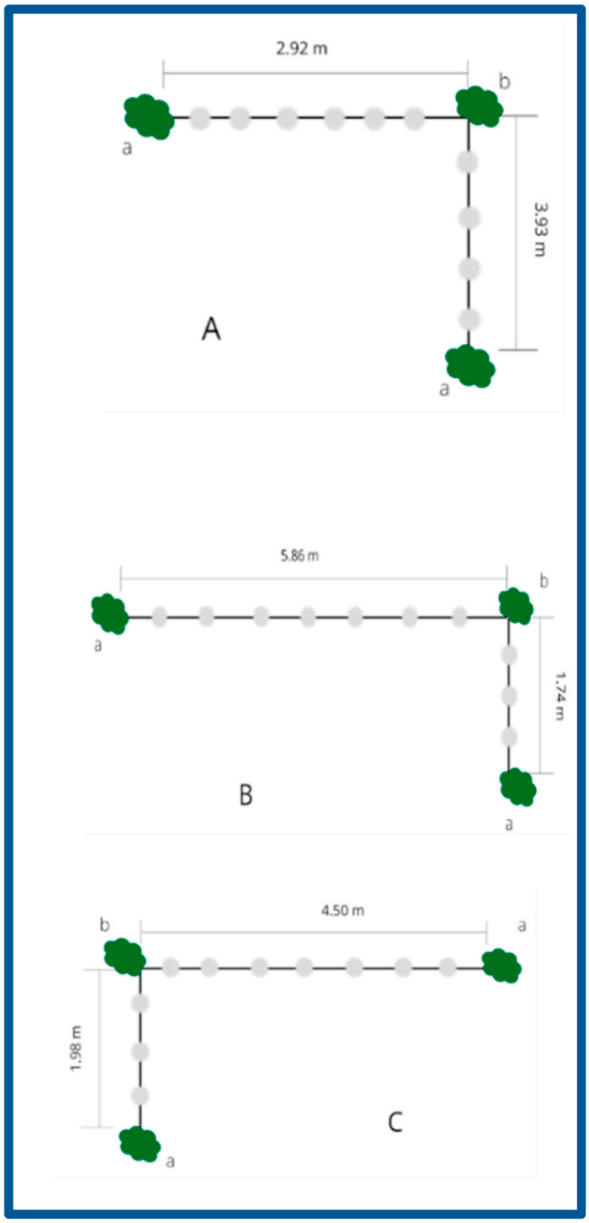

Fig. 5. Scheme of three plots (A, B, C) with total distance between trees for SR measurements. Collars are showed as a gray circles, trees in green. (For interpretation of the references to color in this figure legend, the reader is referred to the Web version of this article.)

2.2.2. Forest inventory

A plot of 1 ha (10,000 m^2) of mangle trees was installed taking as a central point the Jay Zieman (JZ) Eddy Covariance tower (Torre) to perform a classical forest inventory that began on July 26 and culminated on August 24, 2022. For it, the plot was divided into four quadrants of 50 × 50 m, defined by iron rods, and nominated (Am, Az, Mo, Pl (yellow, blue, purple, silver colors in Spanish respectively)), (Fig. 6 shows a scheme). Within the each quadrant all trees greater than or equal to 2.5 cm in DBH were located (x e y coordinates) and the perimeter at breast height (1.30 m aboveground) was measured (at an accuracy of 0.1 cm, Fig. 4). To estimate crown coverage of the trees, a crown diameter estimation is necessary. For it, a sample of 9 trees were selected and crown diameter and DBH were measured (see 2.2.3 section). Table 1 shows the UTM coordinates by GPS MAP 64S, Garmin and Fig. 6 represents the location of the plot. Finally, to estimate the average heigh (Hm, m) and the dominant height (Hd, m; defined as the average height of the 100 tallest trees per hectare [17]) of the mangrove forest stand, we used a lidar mobile terrestrial laser scanner (MTLS, Zeb-Horizon, GeoSLAM ltd., Nottingham, UK), processing the point cloud using AID-FOREST software [18].

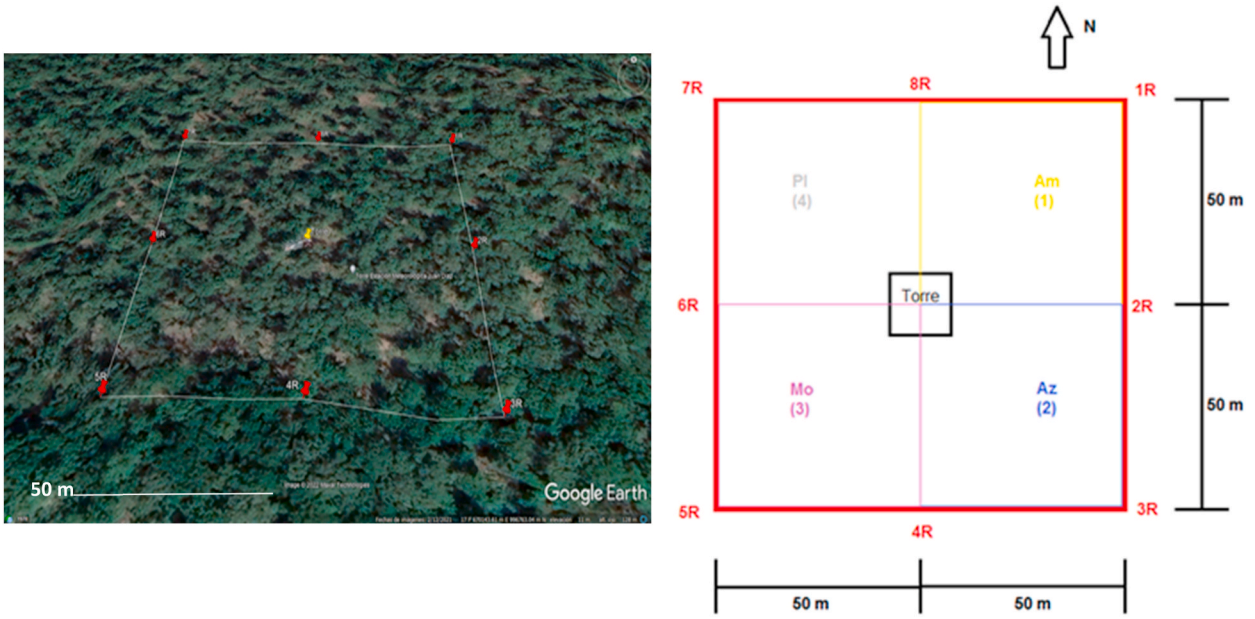

Fig. 6. Location of 1 ha plot. Red marks represent the points. Yellow mark is the JZ tower (Torre). Google Earth. And scheme of the delimitation of the plot by quadrants. (For interpretation of the references to color in this figure legend, the reader is referred to the Web version of this article.)

Table 1
Coordinates of the 8 vertexes of four subplots of the inventory plot (1 ha).

VERTEX	UTM coordinates	
	X (m)	Y(m)
1	670108.43	996847.80
2	670108.43	996797.80
3	670108.43	996747.80
4	670058.43	996747.80
5	670008.43	996747.80
6	670008.43	996797.80
7	670008.43	996847.80
8	670058.43	996847.80

Fig. 7. Path (white line) towards the monitoring sites (red circles). Juan Díaz's mangrove. Source: GPS MAP 64s coordinate data, Garmin. Made in ArcGIS. Google Maps. (For interpretation of the references to color in this figure legend, the reader is referred to the Web version of this article.)

2.2.3. Total soil respiration (SR) experiment

Three plots of (5 × 5 m) were established to monitor the flow of CO_2 emitted from the soil. Fig. 7 shows the location of the three plots: A (9°00′51″ N, 79°27′10″ W), B (9°00′49″ N, 79°27′8″ W) and C (9°00′50″ N, 79°27′5″ W). The measurement sites were chosen because they had certain characteristics that facilitated the measurement process, such as: flat terrain, little water saturation and having a maximum of 2 predominant mangrove trees (*Avicennia bicolor* L and *Avicennia germinans Standl*). In each plot 3 trees were choosen to do SR measurements in a gradient from tree to tree (Fig. 5). Previously, all the DBH and crown diameter (Dc, by averaging the two perpendicular crown diameters) of the 9 sampled trees were measured (Table 2) to define an allometric relationship between the tree crown coverage (Sc, m^2) and diameter at breast height (DBH, cm) for the purpose of estimating the area covered by trees at the hectare level (see 2.2.2 section).

Between the three trees per plot, 10 PVC (Polyvinyl Chloride) collars were placed equidistantly and inserted 3 cm into the soil for SR data collection, (see Fig. 5), using a soil CO_2 flux chamber (Li-6400XT and 6400-09). Measurements with the soil chamber was carried out along 6 different days per plot (A, B, C) in a period from August to November in the rainy season giving a total of 18 different dates, from 8:00 a.m. to 12:00 a.m. Table 3 shows the exact dates and times of the beginning of each measurement and the weather conditions at the site. At times, the ambient humidity and the soil moisture were very high, making it difficult to take soil respiration measurements and, consequently some missing data for some collars did occur (e.g., the collar n° 10 in the C site had not any measurement of SR).

The protocol for measuring CO_2 soil fluxes (efflux, μmol m^{-2} s^{-1}) was as follows. All collars were left in place for the entire study period one month prior to the start of the measurements to avoid effects due to the installation of the collars on efflux. The soil chamber LI-6400-09 has a volume of 991 cm^3 and an area of 71.6 cm^2. Because the soil efflux depends on the CO_2 concentration in the chamber, before starting the measurement the ambient CO_2 concentration on the surface is measured and used as the target. Data are recorded as the soil CO_2 concentration increases into the chamber. The software then calculates by linear regression the appropriate efflux for the ambient concentration (target). This measurement cycle is repeated three times lasting 2–3 min in total and averaged for each collar on each date to subsequently be used to define the SR models.

2.2.4. Environmental measurements

Environmental d'ata (air and soil temperatures, air and soil moistures) were obtained from the Eddy Covariance Meteorological Tower, Jay Zieman (JZ) [19]. This tower is named after Dr. Joseph Zieman (former professor from University of Virginia, USA) who visited Panama in 2008 to tour the Pacific mangroves, encouraged the construction of it to monitor the behavior of the ecosystem and promote its study. The JZ tower is located at coordinates 9°00′51.7″ N, 79°27′10.6″W and has an approximate height of 30 m, and with a measurement radius of 350 m (Fig. 8). It has 8 air temperature sensors (model 41342VC by R. M. Young Company) throughout its structure. Additionally, at different depths (5, 10, 15 and 20 cm) it has soil temperature probes (model 107 by Campbell Scientific Inc.) and soil moisture sensors (10, 20 and 40 cm depths).

2.2.5. Scaling the SR

The extrapolation of the modelled soil respiration measurements taken during the daytime (SR) to the night-time could cause a significant overestimation bias [20]. Published results in other ecosystems (see Ref. [16]) shown that the ratio night-time/day-time SR ranged between 0.61 and 0.84. However, because the mangrove ecosystem is very different from the one mentioned by Martínez et al. (2017) [16], we will not make the SR correction daytime to night-time given the lack of evidence of it in the mangroves. Thus, to scaling SR at plot (1 ha) level, first we need define a model of SR per collar as a function of size of the nearest tree (DBH of the nearest tree to the collar), the distance of the collar to the tree and environmental variables (air o soil temperature and/or soil water content) as predictive variables. Second, applying this model to the 30 collars in the three 5 × 5 plots along the whole period of study using the mentioned predictive variables, we estimated the total soil efflux accumulated by collar (SR_i, $kgCO_2$ $m^{-2}period^{-1}$). Third, to calculate the total efflux under the tree crown per tree for the whole study period ($Efflux_i$, $kgCO_2$ $tree^{-1}$ $period^{-1}$) we extended the efflux per square meter multiplying each accumulate efflux (SR_i) per collar per its influence area under the crown (m^2, see Fig. 9 and equation (1)).

$$Efflux_i = A_{1i}\, x\, SR_{1i} + \sum_{j=2}^{n} A_{ji}\, x \left(\frac{SR_{ji} + SR_{(j-1)i}}{2} \right) \quad (1)$$

Table 2
Mangrove trees species including diameter at breast height (DBH, cm) and crown diameter (Dc, m).

Site	Name	DBH (cm)	Dc (m)
	Avicennia bicolor Standl	44	4.2
A	*Avicennia bicolor Standl*	51	5.1
	Avicennia bicolor Standl	49	4.7
	Avicennia bicolor Standl	48	4.5
B	*Avicennia germinans* L.	62	5.6
	Avicennia bicolor Standl	59	5.4
	Avicennia germinans L.	50	4.8
C	*Avicennia germinans* L.	65	6.2
	Avicennia bicolor Standl	7	1.8

Table 3
Measurement period per site.

Site	Date	Hour (a.m.)	Weather condition	Temperature °C	Humid %
A	4/8/21	10:06:24	Sunny	30	77
	2/9/21	10:40:04	Sunny	30	76
	8/9/21	10:33:17	Rainy	30	78
	14/9/21	9:55:51	Sunny	29	58
	16/9/21	10:08:05	Sunny	28	80
	21/9/21	10:29:20	Sunny	30	79
B	29/9/21	9:40:05	Rainy	27	81
	30/9/21	9:40:15	Sunny	28	83
	12/10/21	9:58:41	Sunny, rainy	28	78
	14/10/21	10:01:50	Sunny	29	80
	19/10/21	9:54:29	Sunny	27	79
	20/10/21	11:06:58	Rainy	28	76
C	27/10/21	10:41:07	Sunny	27	88
	29/10/21	9:59:34	Sunny	29	77
	9/11/21	8:52:11	Partly cloudy	27	81
	11/11/21	8:53:13	Partly cloudy	28	77
	16/11/21	10:24:18	Partly cloudy/rainy	28	75
	17/11/21	10:36:12	Sunny	29	75

Fig. 8. JZ Eddy Covariance Meteorological tower. Juan Díaz's mangrove.

where $Efflux_i$ is the efflux of the tree "i". l_j = distance of each collar "j" to the tree "i"; SR_{ji} is the cumulative efflux along the whole study period ($kgCO_2\ m^{-2}period^{-1}$) for the collar "j" of the tree "i"; A_{ji} is the influence area of each collar "j", i.e., the surface of the circular crown, i.e. $A_1 = \pi l_1^2$; $A_2 = \pi(l_2^2 - l_1^2)$; $A_j = \pi(l_j^2 - l_{j-1}^2)$. We scaled the Efflux to kg of CO_2 per tree in the analyzed period, multiplying the (μmol/s) × (9,368,400 s/period) per (10^{-6} mol/μmol) × (44 g mol^{-1}) × (10^{-3} kg g^{-1}). Fourth, once the $Efflux_i$ emitted by the soil under the tree canopy over the entire period has been calculated, we will define a soil respiration model as a function of DBH using the data from the nine sampled trees. Fifth, this last model will be applied to the DBH distribution of the entire 1ha plot to obtain the total soil CO_2 emitted under tree crowns. Finally, to calculate the total Efflux corresponding to the bare soil we calculated the SR average of those collars out of the tree crown and scaled to total surface of the bare soil at plot level. This surface was obtained as the difference between 10,000 m^2 and the crown coverage by all trees in the plot, i.e. using an allometric relationship to estimate crown projected surface by tree and its DBH applied to the diametric distribution at plot level.

2.2.6. Statistical analysis

To analyse the plot effect (i.e., the three A,B,C, plots) on SR (log-transformed to improve normality and homoscedasticity), a General Linear Model (GLM) [21] was used. The point at which measurements were taken (the collar effect, CE) was also considered as being random in order to consider the repeated measures taken in this experiment. The relationships between SR and DBH, collar distance to the nearest tree and environmental parameters (Tair, Ts and SWC) were defined by multiple regression models, grouped by the factors that affected SR according to the GLM analysis results obtained. All the models were simplified using a forward stepwise regression method based on the general linear test statistic (F-test, [21]). The best models were chosen by selecting the highest R^2, the lowest standard error of estimation (SEE), lack of co-linearity in the predictor variables (low variance inflation factor), and by

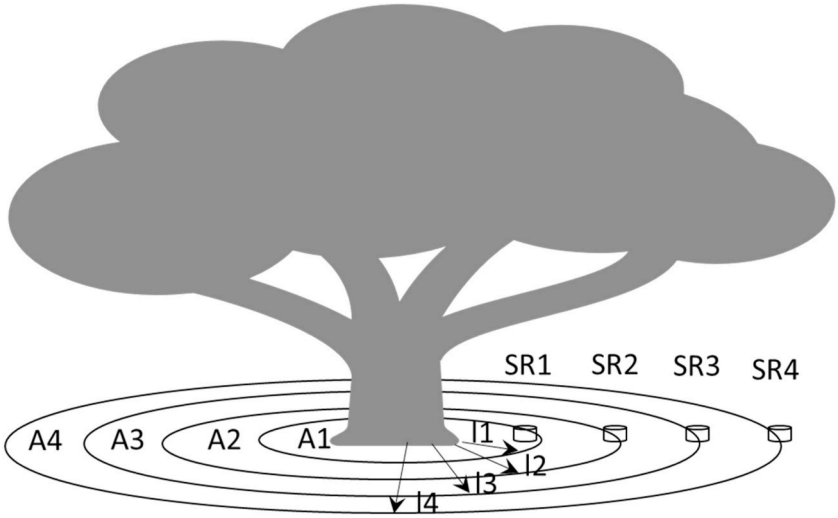

Fig. 9. Methodological scheme to estimate total efflux of the tree "i" ($Effux_i$). Aj is the influence area of each collar j, i.e., the surface of the circular crown; lj = distance of each collar "j" to the stem; SRj is the cumulative efflux along the whole study period ($kgCO_2\ m^{-2}period^{-1}$) of each collar.

graphically analysing the residuals for bias and autocorrelation by computing the Durbin-Watson statistic. Correction for the bias of the regression models as a result of log-transformation of the dependent variables was carried out according to Ref. [22], using CF as the correction factor, where $CF = \exp(SEE^2/2)$ and SEE^2 is the standard error of estimation (residual deviation). Statistical analyses were performed using Statgraphics CenturionXVI software (StatPoint Technologies, Inc., Virginia, USA).

3. Results and discussion

3.1. Forest inventory

Table 4 shows the diameter distribution of the study plot (1 ha) as well as the main forest stand parameters. In spite the low density (less 300 trees ha^{-1} with DBH greater than 7.5 cm, BA < 10 $m^2\ ha^{-1}$) the forest stand had a high average and dominant height that confirms the good site quality. In addition, from the 9 selected trees for SR estimation (Table 2), we defined the tree *Cc* (m^2) vs. DBH (cm) allometric relationship to estimate the crown coverage at plot (1 ha) level. The resulting model was "$Cc(m^2) = 2.172\ \exp(0.0412*DBH(cm))$", $R^2 = 98.6\%$, F = 484.9; p < 0.001. Thus, the crown coverage of all trees within the 1 ha plot resulted on 1680 m^2.

3.2. Environmental conditions

Fig. 10 shows both the changes in soil temperature (15 cm depth) and air temperature along the established research period. The air

Table 4
Diameter distribution at the plot −1 ha-level per specie (*Avicennia bicolor Standl.* and *Avicennia germinans* L.) and total. In addition, basal area (BA), mean quadratic DBH (DBHg), average height (Hm), dominant height (Hd) and total crown coverage of all trees (Cct) were included. CD: diameter class.

CD (cm)	FREQUENCY (trees ha^{-1})							
	Total	*A. bicolor*	*A. germinans*	BA (m^2ha^{-1})	DBHg (cm)	Hm (m)	Hd (m)	Cct (m^2)
5	90	65	25					
10	98	70	28					
15	84	45	39					
20	36	18	18					
25	25	8	17					
30	10	5	5					
35	11	4	7					
40	6	1	5					
45	4	0	4					
50	3	2	1					
55	2	0	2					
60	1	0	1					
65	1	1	0					
Total	371	219	152	9.6	18.2	14.0	17.6	1680
Relative composition		59%	41%					

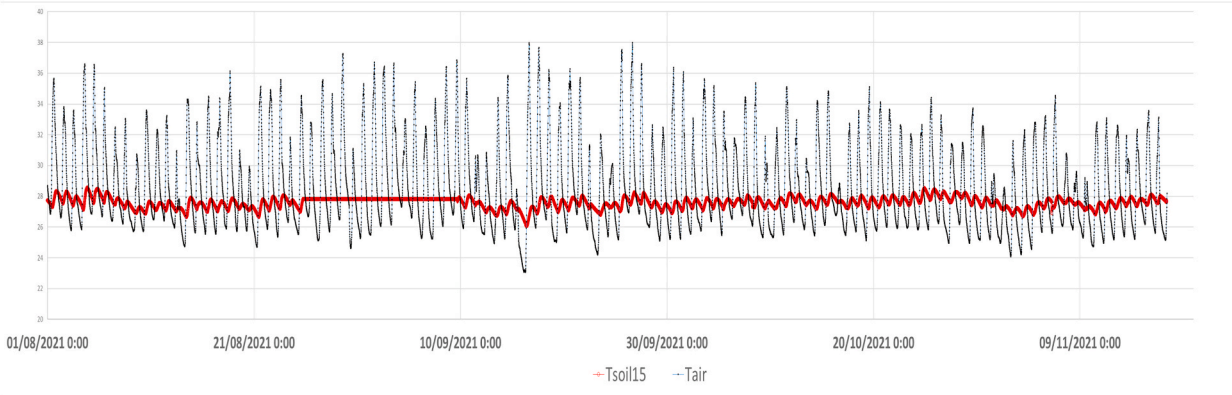

Fig. 10. Air (°C, black line) and Soil (°C, 15 cm depth, red line) temperatures from August 1 to November 17, 2021. (For interpretation of the references to color in this figure legend, the reader is referred to the Web version of this article.)

temperature ranged between a minimum of 23.07 °C and a maximum of 37.97 °C, being the average 28.62 °C. For the soil temperature, the minimum was 26.07 °C and the maximum 28.53 °C, being the average of 27.58 °C. Regarding soil water content (%) the average along the whole period was 39.2 ± 2.9 (%, mean ± standard deviation), i.e., near saturated soil. In general, there was not significant differences between the three sites (A, B, C) regarding to the environmental variables along the study (Fig. 11). Consequently, the variability on SR should be attributed to distance to the tree and uncontrolled factors not measured on the ground.

3.3. Modelling the soil respiration (Efflux) at collar level

Of all the predictor variables tested (*DBH*, distance of the collar to the nearest tree *-Dist-*, air temperature *-Tair-*, soil temperature 15 cm depth *-Tsoil15-*) the statistically significant ones were "*Dist*" and "*Tair*". DBH was not a significant variable, contrary to what was expected and what occurs in other ecosystems. Table 5 show the full and simplified models and their goodness of fit. Thus, the simplified model to be used was:

$$Efflux_i = 6310.4 \ e^{-0.0044 Dist_i - 0.2105 Tair} \quad (2)$$

where $Efflux_i$ (μmol m^{-2} s^{-1}) is the efflux measured in the collar *i*; $Dist_i$ (cm) is the distance of the collar *i* to the nearest tree and *Tair* is the air temperature at the moment of the measurement.

Because we had the temporal series of *Tair* each 10 min for the whole study period, as well as the distance of each collar to nearest tree, we applied Eq. (2) to each collar each 10 min to obtain the average $Efflux_i$ for the entire period. Table 6 shows the average Efflux for each collar under the tree crown along the whole study period. Similarly, the average Efflux for the bare soil was estimated. As can be seen, the averaged Efflux ranged between 5.3 and 6.1 μmol m^{-2} s^{-1} along the whole study period, being higher the closer the collar is to the tree.

3.4. Cumulative total soil respiration (Efflux) under the tree crown

Knowing the average respiration over the study period for each collar, we scaled this SR to the ground surface below the canopy of each tree. For it, we weighted the average Efflux of each collar (Table 6) with its affected surface (Fig. 7) and integrated them according to Eq. (1). Table 7 shows the average Efflux for the soil under the tree crown area (EFFLUXca, μmol s^{-1}) and the total CO_2 emitted per the soil under the projected tree crown area (SRt, kgCO_2) along the study period. Similarly, Table 7 gives too the similar concepts referred to the square meter for the bare soil Efflux. It is obvious that the larger the tree crown, the higher the SR, ranging from 21.4 to 120.4 kg CO_2 along the whole study period (3.5 months).

3.5. Total CO_2 emitted by the experimental plot (1 ha)

To scaling total soil respiration to the 1ha plot along the whole study period, a model relating SRt (kg CO_2 emitted by a tree along the whole study period) and DBH was defined. Table 8 shows the goodness of fit of this model resulting in Eq. (3).

$$SR_t = 5.164 \ DBH^{0.725} \quad (3)$$

where SR_t (kg CO_2 emitted along the whole study period) and DBH (cm, diameter at breast height).

Using this relationship and applying to the diameter distribution, we estimated the total CO_2 emitted by the soil under trees in the experimental plot (1 ha) along the 3.5 months of the study period (Table 9). Similarly, we applied the total CO_2 emitted by the bare soil (Table 7, kg CO_2 m^{-2} along the whole period) by the area of the bare soil (8320 m^2, Table 9). Results showed a total of 33.61 t of CO_2

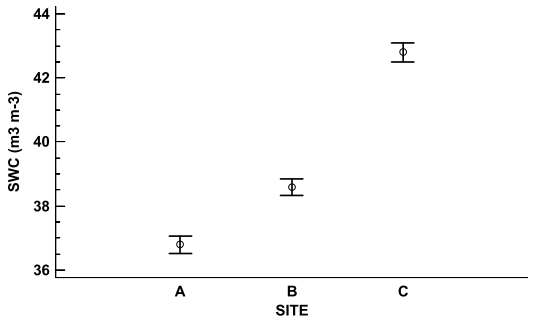

Fig. 11. Significant differences between the three sites (plots 5 × 5 m) in soil water content (SWC).

Table 5
ANOVA for full and simplified regression models regarding efflux estimation at collar level (LOG(Efflux), μmol m^{-2} s^{-1}) depending on predictive variables: DBH (cm), distance of the collar to the nearest tree (Dist, m) and air temperature (Tair, °C). n = 169 measurements. In bold significant coefficients.

FULL MODEL	Sum of Squares	Df	Mean Square	F-Snedecor	Sig. Level	R^2	SEE[a]
Model	26.6547	6	4.44246	8.2	0.0000	20.4	0.74
Residual	87.8169	162	0.54208				
Total (Corr.)	114.472	168					
PREDICTIVE VARIABLES	*Estimate*	*Standard Error*	*t-Student*	*Sig. Level*	*CF*[b]		
CONSTANT	8.4885	1.9533	4.3458	**0.0000**	1.3150		
DBH	0.0008	0.0064	0.1299	0.8968			
Dist	−0.0089	0.0090	−0.9984	**0.3196**			
Tair	−0.2060	0.0594	−3.4678	**0.0007**			
DBH*Dist	0.0000	0.0000	−0.8301	0.4077			
Dist^2	0.0000	0.0001	0.6812	0.4967			
Dist^3	0.0000	0.0000	−0.5808	0.5622			
SIMPLIFIED MODEL	*Sum of Squares*	*Df*	*Mean Square*	*F-Snedecor*	*Sig. Level*	*R^2*	*SEE*[a]
Model	24.8898	2	12.4449	23.06	0	20.8	0.73
Residual	89.5818	166	0.53965				
Total (Corr.)	114.472	168					
PREDICTIVE VARIABLES	*Estimate*	*Standard Error*	*t-Student*	*Sig. Level*	*CF*[b]		
CONSTANT	8.4835	1.8490	4.5882	**0.0000**	1.3053		
Dist	−0.0044	0.0008	−5.2780	**0.0000**			
Tair	−0.2105	0.0587	−3.5831	**0.0004**			

[a] Standard error of the estimation (residual deviation, log-units).
[b] Sprugel (1983) correction factor (already included in the final model, Eq. (3)): CF = exp (SEE^2/2).

ha^{-1} emitted by the soil of the mangrove in 3.5 months, i.e., near 10 t CO_2 per month. As a rule, the soil under tree cover contributes approximately the 39% to the total CO_2 emitted, while bare soil a 64%.

(Gnanamoorthy et al., 2019) found in a study in mangrove area located in India a soil respiration rate estimated about 897 g C m^{-2} $year^{-1}$ (~1 t of CO_2 ha^{-1} monthly) which appears to be characterized by a low soil CO_2 efflux [23]. In our case, near 10 t CO_2 per month. It should be attributed to distance to the tree and uncontrolled factors not measured on the ground. For instance, the soil's temperature, moisture, total carbon content, total nitrogen content, inorganic nitrogen content, bulk density, salinity, redox potential, and microbial population all play a major role in regulating the soil's CO_2 fluxes [23]. Also, high CO_2 efflux is caused by high clay concentration and soil organic carbon content. The high amount of clay content in tropical mangrove forests, which is linked to a higher rate of soil respiration, was also noted in a few studies [23].

Another investigation showed that differences in standing biomass and fine root production are anticipated to have a bigger role in determining C efflux from mangrove sediments than variations in fine root respiration per unit mass [24].

A study in a tropical mangrove forest and a subtropical mangrove forest, the CO_2 efflux rate from carbon wood debris (CWD) respiration was lower than that of soil respiration, but estimation of the CO_2 efflux rate from CWD respiration is still strongly advised for mangrove forests where a significant amount of CWD may occur, for instance because of rising storm intensities. Therefore, our 10 t CO_2 per month value could be explained considering a relatively high CWD respiration contribution. Clarifying the carbon dynamics in climate-vulnerable mangrove ecosystems will be possible with the use of this information [25].

Making a comparison with values presented in studies from other parts of the world where similar equipment was used and with varied methods the difference is remarkable. For instance, doing the respective conversion and estimating the values for the 3 months the value of Mexico is 3.6 ton/ha [26], for India 8.1 ton/ha [23] and the United States 1.9 ton/ha [27] showing that the concentration of CO_2 in the soils of the mangrove of Panama measured in a period of 3.5 months is high.

Table 6
Average of the predicted Efflux each 10 min (μmol m^{-2} s^{-1}) along the whole study period (August 1, 2021, to November 17, 2021) for each collar (a total of 15,614 ten-min periods) and for bare soil.

	DBH tree collar	dist (cm)	μmol m^{-2} s^{-1}
UNDER TREE CROWN	44	24	15.9
	44	87	12.0
	44	154	9.0
	51	21	16.1
	51	39	14.9
	51	91	11.8
	51	95	11.6
	51	162	8.7
	49	23	16.0
	49	121	10.4
	48	26	15.8
	62	23	16.0
	62	42	14.7
	62	85	12.2
	62	125	10.2
	62	220	6.7
	59	34	15.2
	59	113	10.7
	59	195	7.5
	59	274	5.3
	65	27	15.7
	65	44	14.6
	65	105	11.1
	65	166	8.5
	7	32	15.3
	7	93	11.7
	7	151	9.1
	50	38	14.9
	50	97	11.5
BARE SOIL		>200	6.0

Table 7
Average Effux (μmol s^{-1}) per projected tree crown area (EFFLUXca) and total Efflux emitted per the soil under the projected tree crown area (SRt, $kgCO_2$) along the whole study period. Similarly, the average Efflux for bare soil (EFFLUXbs, μmol $m^{-2}s^{-1}$) and the total CO_2 emitted per square meter of bare soil (SRbs, kgCO2 m^{-2} along the whole study period is shown.

TREE DBH (cm)	EFFLUXca (μmol s^{-1})	SRt (kg CO_2 along the whole study period)
44	156.3	64.4
51	210.4	86.7
49	205.6	84.8
48	247.2	101.9
62	234.2	96.6
59	229.8	94.7
65	292.1	120.4
7	51.9	21.4
50	218.7	90.1
	EFFLUXbs (μmol $m^{-2}s^{-1}$)	SRbs (kg CO_2 m^{-2} along the whole study period)
BS	6.00	2.47

Table 8
ANOVA for the regression model regarding to the total CO_2 efflux emitted by the soil under the projected tree crown area (LOG (SRt), (August 1, 2021 to November 17, 2021) depending on the predictive variable (LOG (DBH)), cm), n = 9 trees.

	Sum of Squares	Df	Mean Square	F-Snedecor	Sig. Level	R^2	SEE[a]
Model	1.9890	1	1.9890	136	0.0000	94.4	0.121
Residual	0.1024	7	0.0146				
Total (Corr.)	2.0914	8					
COEFFICIENTS	*Estimate*	*Standard Error*	*t-Student*	*Sig. Level*	*CF*[b]		
CONSTANT	1.6344	0.2365	6.9106	0.0002	1.0073		
LOG (DBH)	0.7254	0.0622	11.6620	0.0000			

[a] Standard error of the estimation (residual deviation, log-units).
[b] Sprugel (1983) correction factor (already included in the final model, Eq. (4): CF = exp (SEE^2/2).

Table 9
Total soil respiration accumulated along the study period for both soil under the projected tree crown area (SRt) and in the bare soil (SRbs) at plot -1ha-level. In addition, tree DBH frequency distribution, crown coverage (Cct) and bare soil coverage (Ccbs) are shown.

CD	Frecuency trees ha^{-1}	Cct (m^2)	SRt ($kgCO_2\ ha^{-1}$)	Ccbs (m^2)	SRbs ($kgCO_2\ ha^{-1}$)	TOTAL SR ($tCO_2\ ha^{-1}$)
5	90	240.2	1494			
10	98	321.4	2689			
15	84	338.5	3093			
20	36	178.2	1633			
25	25	152.1	1333			
30	10	74.8	609			
35	11	101.0	749			
40	6	67.7	450			
45	4	55.5	327			
50	3	51.1	265			
55	2	41.9	189			
60	1	25.7	101			
65	1	31.6	107			
total	**371**	**1680**	**13,038**	**8320**	**20,575**	**33.61**

Keeping absorbed carbon stored in your biomass and soil is the second most important function in mitigating global climate change; mangroves globally contain 1.6% of the total tropical forest biomass, despite only occupying 0.6% of the total tropical forest area. Panama's mangroves have been considered to store an enormous amount of carbon in their upper ground cover, aerial biomass, with an estimated 48 million tons. Likewise, it is estimated that the soil of the Panamanian mangroves stores an additional 29 million tons of carbon [28].

4. Conclusion

The study of carbon dioxide flow in the mangrove of Panama Bay provides information about CO_2 is emitted by the ecosystem at the ground level (heterotrophic and autotrophic breathing). Estimation of CO_2 of the soil value of 33.61 ton/ha in a period of 3.5 months was found.

It appears that the soil respiration of these *Avicennia bicolor Standl.* and *Avicennia germinans L.* species, which are relict species that require legal protection, reflects their singularity.

In conclusion, this research advances our understanding of how soil respiration varies in mangrove forests that thrive in tropical climates.

Author contribution statement

Natasha Alejandra Gómez: Conceived and designed the experiments; Performed the experiments; Analyzed and interpreted the data; Wrote the paper.

Lilisbeth Rodríguez: Conceived and designed the experiments; Performed the experiments; Wrote the paper.

Francisco Ramón López Serrano: Conceived and designed the experiments; Performed the experiments; Analyzed and interpreted the data; Contributed reagents, materials, analysis tools or data; Wrote the paper.

Reinhardt Pinzon: Conceived and designed the experiments; Performed the experiments; Contributed reagents, materials, analysis tools or data; Wrote the paper.

Data availability statement

Data will be made available on request.

Funding

This study was funded by project no. FID2016–30. The funding for which was provided by Secretaría Nacional de Ciencia y Tecnología e Innovación (SENACYT in Spanish) to RP and the APC was funded by contract 27-2022 and through the Sistema Nacional de Investigación (SNI) of SENACYT, and Centro de Estudios Multidisciplinarios en Ciencias, Ingeniería y Tecnología (CEMCIT-AIP). FRLS acknowledge this work co-financed by the National Program for Fundamental Research Projects and NationalProgram for Research, Development and Innovation Oriented to the Challenges of Society (Ref. PID2020-119861RB-I00)

Declaration of competing interest

The authors declare that they have no known competing financial interests or personal relationships that could have appeared to influence the work reported in this paper

Acknowledgment

We thank to MSc. Jaime González, Dr. Nathalia Tejedor, Daniel Nieto and other personnel of the CIHH of Universidad Tecnológica de Panamá for their technical assistance. Also, authors acknowledge the Programa de Saneamiento de Panamá of Ministerio de Salud (MINSA) of Panamá for allows to access at mangrove area where the covariance tower is located and to the Servicio Nacional Aeronaval (SENAN) of Panama for keep our security during the field works. We thank the editor and reviewers for their time and constructive comments, which have helped improve our manuscript.

References

[1] E.J. González Gaudiano, P.Á. Meira Cartea, Educación para el cambio climático ¿Educar sobre el clima o para el cambio? Perfiles Educ. 42 (168) (2020) 157–174. Recuperado el 17 de Febrero de 2022. de, http://www.scielo.org.mx/pdf/peredu/v42n168/0185-2698-peredu-42-168-157.pdf.
[2] J. Trespalacios, C. Blanquicett, P. Carrillo, Gases y efecto invernadero, Instituto Desarrollo Sostenible. Escuela Internacional de Doctorado. Universidad del Norte. SENA. Basilea-Suiza: DSTO. Obtenido de, https://www.academia.edu/38002440/Gases_y_efecto_invernadero, 2018.
[3] ANAM-ARAP, in: A. Tarté (Ed.), Manglares de Panamá: importancia. mejores prácticas y regulaciones vigentes, Primera ed., Novo Art. S.A, Panamá, 2013. Obtenido de, https://online.fliphtml5.com/eebm/lojx/.
[4] MIAMBIENTE y PNUD, Protocolo para medición de carbono en ecosistemas de manglar en Panamá, República de Panamá: Ministerio Federal de Medio Ambiente, 2017.
[5] J. Boone Kauffman, D.C. Donato, M.F. Adame, Protocolo para la medición. monitoreo y reporte de la estructura. biomasa y reservas de carbono de los manglares, CIFOR, Idonesia, 2013.
[6] V.S. Ortega, CONAMA. Obtenido de Humedales por el clima, 2020. http://www.conama11.vsf.es/conama10/download/files/conama2020/CT%202020/5323.pdf.
[7] Wetlands, Wetlands International. Obtenido de Nuevo estudio indica áreas claves de mayor concentración de carbono en la biomasa aérea de los ecosistemas de manglar, 2013. https://lac.wetlands.org/noticia/nuevo-estudio-indica-areas-claves-mayor-concentracion-carbono-la-biomasa-aerea-los-ecosistemas-manglar/#:~:text=Como%20todas%20las%20plantas%2C%20los.en%20hojas%2C%20ra%C3%ADces%20y%20troncos.
[8] R. Cicerone, R. Oremland, Biogeochemical aspects of atmospheric methane, Global Biogeochem. Cycles (1988) 288–327. https://doi.org/10.1029/GB002i004p00299.
[9] Ley 1 de 2 de febrero de 2015. (s.f.). Que declara área protegida al refugio de vida silvestre Sitio Ramsar Humedal Bahía de Panamá. (L. A. Nacional. Ed.) Panamá: Gaceta Oficial Digital. Obtenido de https://www.asamblea.gob.pa/APPS/LEGISPAN/PDF_NORMAS/2010/2015/2015_615_4009.pdf.
[10] T. Stith, Gower, Patterns and Mechanisms of the Forest Carbon Cycle, in: Annual Review of Environment and Resources, 2003. https://www.annualreviews.org/doi/abs/10.1146/annurev.energy.28.050302.105515.
[11] F.A.G. Morote, M.A. Abellán, E. Rubio, E.M. García, F.G. Saucedo, M.I.P. Córdoba, F.R.L. Serrano, Productivity and seasonality drive total soil respiration in semi-arid Juniper Woodlands (Juniperus thurifera L., southern Spain), Forests 13 (2022) 538, https://doi.org/10.3390/f13040538.
[12] L. Sugasti, R. Pinzón, First approach of abiotic drivers of soil CO_2 Efflux in Barro Colorado Island. Panama, Air Soil. Water Res. 2020 (2019) 13, https://doi.org/10.1177/1178622120960096.
[13] J. Lloyd, J. Taylor, On the temperature dependence of soil respiration, Funct. Ecol. (1994) 315–323.
[14] K.W. Kaufmann, Nuestros Humedales. Nuestro Futuro. Plan de Conservación para los Humedales de la bahía de Panamá (Primera ed.). Panamá: Sociedad Audubon de Panamá, 2012.
[15] G. Cárdenas-Castillero, Centro de Incidencia Ambiental de Panamá. Entorno socioambiental y calidad de agua del Área Protegida Humedal Bahía de Panamá vol. 27, Fundación David & Lucile Packard, Panamá, 2018.
[16] E. Martínez-García, F.R. López-Serrano, T. Dadi, F.A. García-Morote, M. Andrés-Abellán, Pumpanen, E. Rubio, Medium-term dynamics of soil respiration in a Mediterranean mountain ecosystem: the effects of burn severity, post-fire burnt-wood management, and slope-aspect, Agric. For. Meteorol. 233 (2017) 195–208, https://doi.org/10.1016/j.agrformet.2016.11.192.
[17] J. Pardé, J. Bouchon, Dasometría. Versión española de Dendrométrie. Ecole Nationale de Génie Rural des Eaux et Forêts, ENGREF), Madrid, 1994.
[18] F.R. López-Serrano, E. Rubio, Garcia Morote Francisco, Abellán Manuela, Picazo Marta, Saucedo Francisco, Martínez García Eduardo, J. Innerarity, L. Lucas, O. González, J.C. González, Artificial intelligence-based software (AID-FOREST) for tree detection: a new framework for fast and accurate forest inventorying using LiDAR point clouds, Int. J. Appl. Earth Obs. Geoinf. 113 (2022), 103014, https://doi.org/10.1016/j.jag.2022.103014.
[19] R. Pinzón, PROYECTO FID16-30: "Análisis de flujos de CO_2 y vapor de agua de un ecosistema de manglar en la bahía de Panamá", in: INFORME: PARÁMETRO DE TEMPERATURA DEL SUELO PARA EL AÑO 2018, SENACYT UTP FID16-30, Panamá, 2018. http://manglar-carbono.utp.ac.pa/. accessed on 20 July 2022.
[20] E.A. Davidson, K. Savage, L.V. Verchot, R. Navarro, Minimizing artifacts andbiases in chamber-based measurements of soil respiration, Agric. For.Meteorol. 113 (1–4) (2002) 21–37. https://harvardforest1.fas.harvard.edu/sites/harvardforest.fas.harvard.edu/files/publications/pdfs/Davidson_AgriForestMeterology_2002a.pdf.
[21] J. Neter, M.H. Kutner, C.J. Nachtsheim, W. Wasserman, Applied Linear Statistical Models, fourth ed., Irwin, Chicago, 1996.
[22] D.G. Sprugel, Correcting for bias in log-transformed allometric equations, Ecology 64 (1) (1983) 209–210, https://doi.org/10.2307/1937343.
[23] P. Gnanamoorthy, Diurnal and seasonal patterns of soil CO_2 efflux from the Pichavaram mangroves. India, Environ. Monit. Assess. (2019) 191–258, https://doi.org/10.1007/s10661-019-7407-2.
[24] E. Catherine, Lovelock and others, Fine root respiration in the mangrove Rhizophora mangle over variation in forest stature and nutrient availability, Tree Physiol. 26 (12) (2006) 1601–1606, https://doi.org/10.1093/treephys/26.12.1601.
[25] S. Umnouysin, et al., Comparative carbon dioxide efflux rates from respiration of coarse woody debris among three mangrove species in Thailand, Tropics 26 (2017) 49–57, https://doi.org/10.3759/tropics.MS16-16.
[26] A. Quintero, W. Plata, V. Olimón, S. Monjardín, X. Nemiga, Dynamics of changes in land use and estimation of CO_2 in mangroves in the Marismas Nacionales area. Mexico, Cienc. Mar. (2021) 105–125.
[27] L. Simpson, T.Z. Osborne, I.C. Feller, Wetland Soil CO_2 Efflux Along a Latitudinal Gradient of Spatial and Temporal Complexity, Estuaries and Coasts 42 (2019) 45–54. https://doi.org/10.1007/s12237-018-0442-3.
[28] MIAMBIENTE, Mitigación del Cambio Climático: Sumidero de Carbono, Obtenido de Manglares y el Cambio Climático, 2015, https://manglares.miambiente.gob.pa/index.php/classifieds/category-news-2/category-news-4.